

PACS numbers: 42.55.Wd; 42.60.Da; 07.60.Ly
DOI: 10.1070/QE2013v043n08ABEH015143

Selection of linear-cavity fibre laser radiation using a reflection interferometer

V.S. Terentyev, V.A. Simonov

Abstract. **We consider the use of a two-mirror multibeam reflection interferometer as a selector of linear-cavity single-mode fibre laser radiation and present experimental data on continuous wavelength tuning of an erbium-doped fibre laser. Conditions are found for single-longitudinal-mode operation of the fibre laser cavity using a reflection interferometer, with the possibility of broadband wavelength tuning.**

Keywords: *multibeam reflection interferometer, fibre laser, mode selection, single-longitudinal-mode lasing.*

1. Introduction

Multibeam two-mirror reflection interferometers (RIs) may probably offer a record-high degree of radiation selection among conventional reflected-light spectral selectors, such as two-mirror interferometers and diffraction gratings [1]. The configuration of the RI cavity is identical to that of the Fabry–Perot interferometer (FPI): two mirrors some distance apart. One distinctive feature of the RIs is that their input mirror, facing the light source, contains a component that causes considerable losses in a travelling light wave. Owing to this, however, the reflected-light spectral characteristics of the RIs can be very similar to the transmission characteristics of the FPI. In contrast to that of the FPI, the spectral profile of the response function of the RIs, determined by the structure of their input mirror, can be varied to some extent [2]. The RIs are easy to fabricate owing to the simple design of their two-mirror cavity: an RI can be produced through vacuum deposition of thin layers on a substrate or fibre. There are several widely used state-of-the-art techniques for selecting the radiation of single-mode fibre lasers and laser diodes with a waveguide structure. One of them employs fibre Bragg gratings (FBGs) with a narrow spectral reflection peak [3]. However, the limited transverse spatial coherence of laser beams for FBG inscription adds complexity to the fabrication of gratings with a spectral width less than 0.1 nm. To achieve single-longitudinal-mode lasing, use is also made of distributed feedback cavities [4]. These methods, however, are unsuitable for rapid (over 10^2 Hz) wavelength scanning in a wide spectral range (about 100 nm).

V.S. Terentyev, V.A. Simonov Institute of Automation and Electrometry, Siberian Branch, Russian Academy of Sciences, prosp. Akad. Koptyuga 1, 630090 Novosibirsk, Russia;
e-mail: terentyev@iae.nsk.su, visimonov@gmail.com

Received 8 February 2013; revision received 12 March 2013
Kvantovaya Elektronika **43** (8) 706–710 (2013)
Translated by O.M. Tsarev

Another selection technique employs a fibre-optic FPI together with an optical isolator in the cavity of a ring laser [5]. One drawback to this approach is that it is difficult to ensure a small cavity length, which influences the number of generated modes in the spectral range of selection of fibre-optic FPIs. It is worth mentioning a four-mirror configuration [6], where the cavity of a laser diode is 'split' into two cavities slightly differing in length. The cavities are several microns apart. The difference in eigenfrequency between the cavities is such that, in the free spectral range of the entire system, only one eigenmode can be generated within the amplification line, which offers the possibility of rapidly tuning the output wavelength over 15 nm.

Selection with an RI has the advantage of using reflected light, which allows one to simultaneously select only one cavity frequency and have a broad spectral range and high speed of radiation tuning. The main purposes of this study is to demonstrate radiation selection in a linear-cavity fibre laser using an RI.

2. Response function of the RI

To assess the degree of mode selection, it is necessary to consider the response function of the RI in reflection, which is more complex than that of the FPI. The properties of the fibre-integrated, thin metallic film-based RI used in our experiments (Fig. 1) can be described rather accurately by three-dimensional theory in the plane wave approximation [7]. In the light reflected from the interferometer, the ray reflected from the input mirror outside the cavity interferes

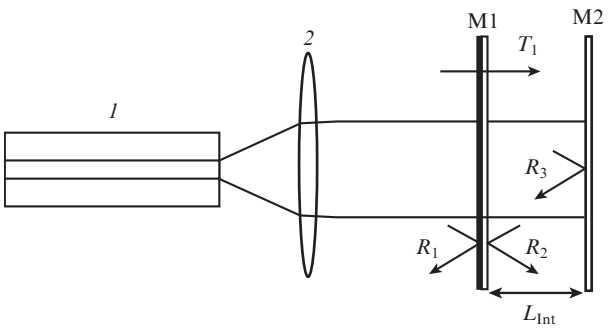

Figure 1. Schematic of the fibre-integrated RI: (*1*) SMF-28e fibre, (*2*) collimator (8-mm focal length), (M1) input mirror based on a thin metallic film and multilayer dielectric coating (with reflectances $R_1 \ll R_2$ and transmittance $T_1 > 0$), (M2) end mirror (reflectance $R_3 = 1$). L_{Int} is the RI base length.

with the ray leaving the cavity. Generally, the response function can be written in the form

$$\tilde{R}(\varphi) = R_1 + 2T_1\sqrt{R_1R_3}\,\frac{\cos(2\varphi+\vartheta)-\sqrt{R_2R_3}\cos\vartheta}{1+R_2R_3-2\sqrt{R_2R_3}\cos(2\varphi)} + \frac{T_1^2R_3}{1+R_2R_3-2\sqrt{R_2R_3}\cos(2\varphi)}, \quad (1)$$

where $R_{1,2}$ and $T_{1,2}$ are the reflectances and transmittances of mirror M1 (R_2, inside the cavity; $T_1 = T_2$) and R_3 is the reflectance of mirror M2 (Fig. 1). Let $\Psi_{1,2,3}$ and $\Phi_{1,2}$ be, respectively, the phases of the reflection and transmission coefficients of the mirrors ($\Phi_1 = \Phi_2$). We have $\vartheta = \Psi_1 + \Psi_2 - 2\Phi_1$, $\varphi = 2\pi L_{\rm Int}/\lambda - (\Psi_2 + \Psi_3)/2$ (where φ is the phase shift per pass between the mirrors; $L_{\rm Int}$ is the RI base length; and λ is the wavelength of the light). For a clear analytical description of lasing conditions, relation (1) can be significantly simplified by using parameters of an asymmetric diffraction mirror [8]:

$$R_1 = 0, \Psi_1 = 0, \quad 0 < R_2 < 1, \qquad \Psi_2 = \pi, \quad T_{1,2} = (1-R_2)/2, \quad \Phi_{1,2} = \pi/4, \quad (2)$$

where the coefficients are taken only for zeroth-order diffraction. Such a mirror has strong asymmetry in its reflectances ($R_1 \ll R_2$) and always causes losses in a travelling light wave because some of the light is scattered through diffraction ($R_2 + T_2 < 1$). The end mirror of the RI is highly reflective: $R_3 = 1$, $\Psi_3 = \pi$. Relation (1) then takes the form

$$\tilde{R}(\varphi) = \frac{R_{\max}}{1+H\sin^2\varphi}, \qquad R_{\max} = \frac{(1+\sqrt{R_2})^2}{4}, \quad H = \frac{4\sqrt{R_2}}{(1-\sqrt{R_2})^2}, \quad (3)$$

where $R_{\max}$ is the maximum reflectance of the RI and H is its coefficient of finesse. Relation (3) is equivalent in structure to the transmitted-light response function of the FPI. The relation for $R_{\max}$ shows that $\tilde{R}(\varphi) < 1$ at any $R_2 < 1$. For $R_2 \to 1$, we have $\tilde{R}(\varphi) \to 1$, so it is more beneficial to use high-finesse cavities. By analogy with the FPI, the interference fringe finesse of the RI can readily be expressed through the coefficient of finesse: $F = \pi\sqrt{H}/2$.

3. Radiation selection experiments

The first radiation selection experiments with the use of a fibre laser RI were performed in a linear cavity ytterbium fibre laser [9]. The laser wavelength was tuned in a narrow range (20 GHz, 0.1 nm at a wavelength of 1080 nm) corresponding to a high reflectance of the cavity mirror – a fibre Bragg grating (an RI with a low-finesse cavity was used). The use of a fibre-integrated, thin metallic film-based RI (Fig. 1) having a high-finesse cavity allowed us to obtain considerably broader tuning ranges. In particular, in experiments with an erbium-doped fibre ring laser [7], wavelength tuning over 40 nm was demonstrated. However, the use of an RI for mode selection in a ring cavity has essentially no serious advantages over conventional selection techniques, e.g. with the use of a fibre-optic FPI placed in the cavity of a ring laser together with a fibre-optic Faraday isolator for reflected-light suppression [5]. Reflected-light operation of the RI seems to have advantages only in a linear-cavity configuration.

To demonstrate wavelength tuning with a fibre-integrated RI, we used a linear-cavity erbium-doped fibre laser operating near 1550 nm (telecom window). The spectral properties of the fibre-integrated RI in this range were studied at different $L_{\rm Int}$ values (Fig. 2). The interferometer was exposed to broadband spontaneous emission from the erbium fibre laser in subthreshold mode through a fibre-optic circulator. Reflection spectra were measured at the output port of the circulator using a spectrum analyser. For continuous wavelength tuning, we varied the RI base length (the end mirror was scanned using piezoceramic). The tuning rate of the maximum reflectance of the RI in this configuration with nonfibre components was up to 500 s^{-1}. The maximum interference fringe finesse was determined to be $F = 40$, and the maximum reflectance was $R_{\max} \approx 0.5$. This points to appreciable light losses at the interface between the bulk components and fibre optics. The ratio of the maximum to minimum reflectance was $R_{\max}/R_{\min} = 40$. Reducing the mirror separation allowed us to obtain a free spectral range of up to 120 nm ($L_{\rm Int} \approx 10^{-5}$ m). It can be broader and is limited by the spectral width of the reflectance of the mirrors, like in the case of the FPI. The lowest reflectance, determined by the reflection from the fibre end face (Fig. 1), was rather high ($R_{\min} = 0.025$) and had a significant effect on the spectral tuning range of the laser. The problem of contrast arises here because of the imperfect fabrication of the components of the RI. In theory, the RI may have perfect contrast, which is in principle unachievable with the FPI [1].

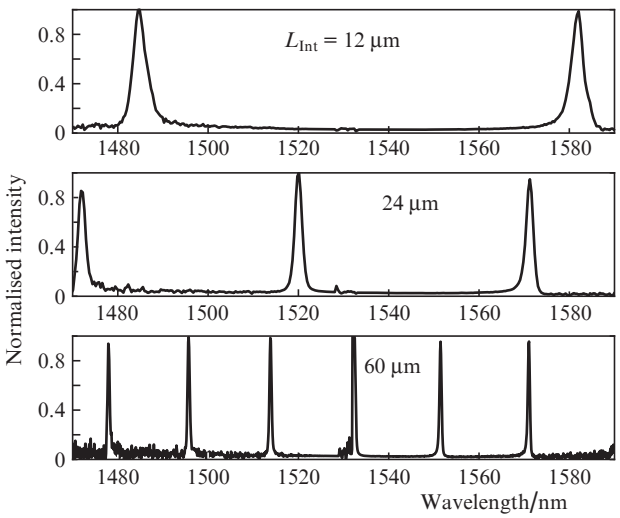

Figure 2. Normalised reflection spectra of the RI exposed to spontaneous emission from a laser in subthreshold mode at $L_{\rm Int}$ = 12, 24 and 60 μm.

The laser was pumped by a single-mode laser diode (*3*) (980-nm wavelength, 150-mW maximum power) through a wavelength-division multiplexer (*4*) located in the cavity (Fig. 3). The total cavity length was 10 m, and the erbium-doped fibre length was 4.5 m (*5*). The passive section of the cavity was made of SMF-28e fibre. Since these fibres differ in fundamental-mode diameter, the fusion splices (denoted by

crosses) always caused wavelength-dependent losses (about 0.5 dB), reducing the cavity finesse. The loss was doubled when the laser wavelength was stabilised by a saturable absorber (*2*) in the form of an unpumped 12-cm-long active fibre. The beam was extracted from the cavity through a 80/20 fibre coupler (*6*). A broadband mirror (*8*) with 70% reflectance was made on the fibre end face. Our measurements showed that the small-signal absorption in the active fibre was 3 dB m^{-1} (1530 nm) and the pump absorption was 4.3 dB m^{-1} (980 nm).

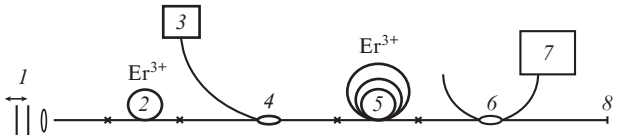

Figure 3. Schematic of a linear-cavity fibre laser: (*1*) fibre-integrated RI, (*2*) saturable absorber (0.12 m long), (*3*) single-mode pump diode (980 nm, 150 mW), (*4*) wavelength-division multiplexer, (*5*) erbium-doped active fibre (4.5 m long), (*6*) fibre coupler (80/20 coupling ratio), (*7*) optical spectrum analyser, (*8*) dielectric mirror (70% reflectance).

For approximate mathematical modelling of lasing characteristics (power, lasing threshold and efficiency) in a model proposed by Barnard et al. [10], we used the spectral distributions of the pump and signal absorption and emission cross sections reported by Miniscalco [11] for an Al/P-silica fibre. Those data were also used to calculate the spectral dependences of the pump and signal saturation powers, which were normalised to the values measured at wavelengths of 980 and 1547 nm. The calculation results agreed well with experimental data: the key characteristics of the laser – output power, slope efficiency and tuning range – coincided to within one order of magnitude at the measured losses and gain medium, scheme and pump parameters. This was interpreted as evidence that the theory could be used to calculate the characteristics of the selector needed for single-longitudinal-mode lasing in a short-cavity laser.

When the reflection peak of the RI (*1*) was tuned by more than 20 nm, parasitic lasing occurred near the peak gain wavelength of the medium (1530 nm), which was due to the low contrast of the RI response function. Taking into account the parasitic lasing, we optimised the interferometer base length so that the maximum tuning range and the degree of radiation selection corresponded to a 20-nm free spectral range (Fig. 2, lowermost spectrum). At this RI base length, a fringe finesse of 40 was reached, whereas at lower L_{Int} values it dropped to 30.

The laser output was multimode because a large number of longitudinal modes fell in the spectral range of the high reflectance of the RI. The number of generated modes can be estimated as

$$N_{\mathrm{mod}} \sim Ln/(L_{\mathrm{Int}}F), \tag{4}$$

where n is the reflective index of the fibre material and L is the cavity length. We obtained $N_{\mathrm{mod}} \sim 10^3$, which leads to competition between longitudinal modes and temporal laser wavelength instability, e.g. because of the spatial hole burning in the gain medium of the laser.

Figure 4 shows laser output spectra obtained with a Yokogawa AQ 6370 spectrum analyser (Fig. 3) in three regions (1525.5, 1533 and 1542 nm) within the tuning range. There are two spectra in each region, which points to spectral lasing instability. Longitudinal modes were generated within 0.1 nm. To reduce the lasing instability due to spatial hole burning in linear-cavity lasers, use is commonly made of a saturable absorber. In our case, this led to no significant narrowing of the spectrum but improved temporal lasing stability. In addition, this reduced the wavelength tuning range, output power and laser efficiency. The spectra in Fig. 4 were obtained with no saturable absorber. An individual mode is represented by a characteristic profile with a full width at half maximum (FWHM) equal to the minimum spectral resolution of the spectrum analyser (20 pm). Within this interval, few-mode lasing is possible.

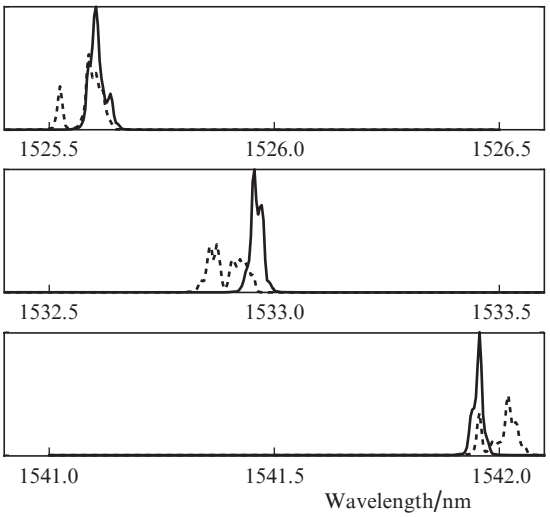

Figure 4. Laser output spectra in three regions (two spectra in each region).

The maximum tuning range with no saturable absorber was about 20 nm. The RI base length corresponding to this interval (to the free spectral range) was 60 μm, and the FWHM of the reflection band of the RI was 0.5 nm. We failed to obtain a broader tuning range because of the insufficient contrast of the response function of the interferometer. A broader tuning range can be achieved by controlling the cavity finesse using the spectral properties of the mirror (*8*), thereby effectively reducing the influence of the contrast of the maximum gain profile of the active medium within the free spectral range of the RI. The highest slope efficiency of the laser was about 5%. The output power per coupler port was up to 1 mW (depending on pump power).

The linear laser configuration (Fig. 3) allows one to exclude two optical components from the cavity: the wavelength-division multiplexer (*4*) and fibre coupler (*6*). The active fibre core is then pumped not in the cavity but outside, through the mirror, and the lasing output is extracted through a wavelength-division multiplexer (Fig. 5). This allows one to markedly reduce the cavity length and increase the mode spacing. If a selector possesses sufficient selection sharpness, it may ensure lasing at only one eigenfrequency of the cavity within the gain band of the fibre laser. It seems likely that the fibre-integrated RI employed in our experiments cannot be

used in such a configuration because the cavity length cannot be made smaller than the focal length of the collimator. In such a configuration, a fibre-optic RI [12], which is thought to be in a sense a fibre-optic analogue of a multibeam phase interferometer [13, 14], can serve as a selector. The spectral properties of mirrors M, M1 and M2 should ensure appropriate lasing conditions. It is desirable that the mirrors be broadband and highly reflective. They can be made as thin-film coatings on the fibre end faces by vacuum deposition. The fibre cavity of a variable-base-length RI can be fabricated by the same methods as are used to make fibre-optic Fabry–Perot cavities (see e.g. Refs [15, 16]).

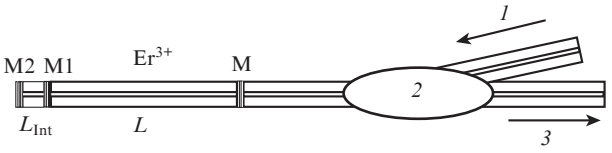

Figure 5. Schematic of a short linear cavity fibre laser: (*1*) pump beam, (*2*) wavelength-division multiplexer, (*3*) laser output, (M) cavity mirror, (M1) input mirror of the RI (asymmetric in its reflectances), (M2) highly reflective end mirror of the RI. L is the laser cavity length and $L_{\rm Int}$ is the RI base length.

4. Single-longitudinal-mode lasing conditions

Conditions for single-longitudinal-mode operation of fibre lasers can be inferred from an analytical model proposed by Barnard et al. [10]. According to these conditions, within the gain band of the active laser medium the loss level for all other modes should exceed their gain level, i.e. they should be in the subthreshold regime. In the case of gas lasers with a small gain coefficient, even small mode discrimination according to the loss level may ensure conditions for single-longitudinal-mode lasing [17]. We apply this approach to solid-state lasers, which have a large gain coefficient in a broad spectral range. Conditions for the eigenfrequencies of the laser cavity (Fig. 5) can be derived from the equation of phase matching of light waves:

$$2\left(\frac{2\pi Ln}{\lambda}-\frac{\Psi_{\rm M}+\Psi_{\rm Int}(\lambda)}{2}\right)=2\pi m, \tag{5}$$

where $\Psi_{\rm M}$ is the phase of reflection from mirror M; $\Psi_{\rm Int}$ is the phase of reflection from the RI, and $m = 1, 2, 3, \ldots$ It follows from the theory of RIs [1] that the phase of the RI in case (2) can be written in the form

$$\Psi_{\rm Int}(\lambda)=\frac{\pi}{2}-\arctan\left(\frac{\sin(2\psi)}{\cos(2\psi)-\sqrt{R_2}}\right), \tag{6}$$

where $\psi = 2\pi nL_{\rm Int}/\lambda$. Consider in frequency space, $\nu = c/\lambda$, two neighbouring longitudinal laser modes of order m and $m + 1$ with frequencies $\nu_m = \nu_0$ and $\nu_{m+1} = \nu_0 + \delta\nu$, $\delta\nu/\nu_0 \ll 1$ (ν_0 is the resonance frequency of the RI and is the frequency spacing between the laser cavity modes). Subtracting the corresponding Eqns (5) from each other, expanding the difference in terms of the small parameter $\delta\nu/\nu_0$ and retaining only the first-order terms, we obtain

$$\delta\nu\approx\frac{c}{2Ln}\frac{1+R_2-2\cos(2\psi_0)\sqrt{R_2}}{[1+L_{\rm Int}/L]+R_2-[2+L_{\rm Int}/L]\cos(2\psi_0)\sqrt{R_2}}, \tag{7}$$

where $\psi_0 = 2\pi nL_{\rm Int}\nu_0/c = \pi$ is the resonance phase of the RI. Since $L_{\rm Int}/L \ll 1$, let us expand (7) in terms of this small parameter:

$$\delta\nu\approx\frac{c}{2Ln}\left(1-\frac{L_{\rm Int}}{L}\frac{1}{1-\sqrt{R_2}}\right). \tag{8}$$

Equation (8) shows that the eigenfrequencies are concentrated around the resonance frequency of the selector (in contrast to the case of undisturbed cavities [17]), which is characteristic as well of an FPI in a ring cavity. The degree of concentration is determined by the relationship between the cavity length and RI fringe finesse, and conditions for lasing at one frequency within the free spectral range may have the following form:

$$\begin{aligned} &G_{\max}^2T_{\rm r}^2R_{\rm M}R_{\max}\geqslant 1,\\ &G_{\max}^2T_{\rm r}^2R_{\rm M}R_{\delta\nu}<1,\\ &G_{\max}^2R_{\min}<G_{\min}^2R_{\max}\geqslant 1, \end{aligned} \tag{9}$$

where $G_{\max,\,\min}$ are extrema in the spectral profile of the maximum gain within the free spectral range of the RI; $R_{\rm M}$ is the reflectance of the laser cavity mirror; $T_{\rm r}$ is the single-pass transmittance of the cavity; $R_{\max} = \tilde{R}(\psi_0)$ and $R_{\min} = \tilde{R}(\psi_0 + \pi/2)$ are the maximum and minimum reflectances of the RI; $R_{\delta\nu} = \tilde{R}(\psi_0 + \delta\psi)$; and $\delta\psi = 2\pi nL_{\rm Int}\delta\nu/c$. Inequalities (9) impose limitations on characteristics of the response function. They are derived under the assumption that the $R_{\rm M}T_{\rm r}^2$ product is wavelength-independent in the free spectral range of the RI. The first inequality requires $R_{\max}$ values as high as possible; the second requires a high degree of selection, i.e. high fringe finesse F; and the last requires high contrast.

For estimates in the $L_{\rm Int} \ll L$ approximation, the eigenmodes of the three-mirror cavity (Fig. 2) can be taken to be undisturbed, i.e. $\delta\nu = c(2Ln)^{-1}$. Then, from (9) we obtain a condition for the fringe finesse F:

$$F>\frac{\sqrt{G_{\max}^2T_{\rm r}^2R_{\rm M}-1}}{\pi}\frac{L}{L_{\rm Int}}. \tag{10}$$

Under certain conditions, the square root in the numerator in (10) can be less than unity and diminish requirements for F, which is characteristic of gas lasers with small gain coefficients. According to (10), the interference fringe finesse required for the laser configuration under consideration (Fig. 2) is $F > 10^4$. Calculations show that, in the case of the active fibre used, in the short-cavity configuration (Fig. 5) with $L = 0.1$ m and $L_{\rm Int} = 10^{-4}$ m, single-mode lasing can be obtained at finesses in the range 10^2–10^3. The free spectral range in silica fibre, i.e. the laser wavelength tuning range, will then be about 7.5 nm. The use of fibres with a larger gain coefficient (for example, EDFC-980-HR; 80 dB m^{-1} at 1530 nm) or operation in other spectral ranges, where gain coefficients much greater than unity are possible, will allow one to further reduce the cavity length, diminish requirements for F and ensure a tuning range over 50 nm. The RI method is applicable to semiconductor lasers with a cavity length less than 1 mm. The finesse necessary for this is $F < 10^2$.

In the case of a previously proposed fibre selector with a spatially symmetric structure [12], simultaneous lasing at two orthogonal polarisations is possible. The fibre-optic RI method makes it, in principle, possible to include a polarisation selector in the structure of the input mirror if one polarisation should be separated out.

5. Conclusions

A fibre-integrated, thin metallic film-based RI has been successfully used to continuously tune the emission wavelength of a linear-cavity erbium-doped fibre laser. We have analytically examined the possibility of mode selection with an RI for achieving single-longitudinal-mode operation of a single-mode fibre laser. We expect that using an all-fibre RI will considerably reduce the reflection loss, increase the contrast of the response function and improve the interference fringe finesse. At the present stage, available processes for the fabrication of fibre-optic thin metallic film-based RIs allow them to be used in low-power lasers (no more than 20 μW). Light absorption in the film may degrade the characteristics of the asymmetric mirror above a certain incident intensity. The fibre-integrated RI schematised in Fig. 1 possesses a considerably higher optical damage threshold (up to 200 mW), because the beam diameter in this configuration is two orders of magnitude larger than that in the all-fibre configuration. The use of scattering dielectric structures in fibre [12] will enable an increase in the optical damage threshold of RIs.

Acknowledgements. This work was supported by the RF Ministry of Education and Science (Grant No. P1264, 9 June 2009 and No. 14.132.21.1669, 1 October 2012) and the Physical Sciences Division and Presidium of the Russian Academy of Sciences.

References

1. Troitskii Yu.V. *Mnogoluchevye interferometry otrazhennogo sveta* (Multibeam reflected-light interferometers) (Novosibirsk: Nauka, 1985).
2. Terent'ev V.S. *Avtometriya*, **45** (6), 89 (2009).
3. Song W., Havstad Y.A., Starodubov S.D., et al. *IEEE Photonics Technol. Lett*., **13** (11), 1167 (2001).
4. Hunsperger R.G. *Integrated Optics. Theory and Technology* (New York: Springer, 2009).
5. Zyskind L., Sulhoff J.W., Stone J.J., et al. *Electron. Lett.*, **27** (21), 1950 (1991).
6. Tsang W.T., Olsson N.A., Logan R.A. *Appl. Phys. Lett*., **42** (8), 650 (1983).
7. Terent'ev V.S., Simonov V.A. *Avtometriya*, **47** (4), 41 (2011).
8. Kol'chenko A.P., Terent'ev V.S., Troshin B.I. *Opt. Spektrosk.*, **101** (4), 674 (2006).
9. Babin S.A., Kablukov S.I., Terentiev V.S. *Laser Phys.*, **18** (11), 1241 (2008).
10. Barnard C., Myslinski P., Chrostowski J., Kavehrad M. *IEEE J. Quantum Electron*., **30** (8), 1817 (1994).
11. Miniscalco W.J. *J. Lightwave Technol.*, **9** (2), 234 (1991).
12. Terent'ev V.S. *Avtometriya*, **48** (4), 41 (2012).
13. Bel'tyugov V.N., Troitskii Yu.V. *Kvantovaya Elektron*., **2** (2), 391 (1975) [*Sov. J. Quantum Electron*., **5** (2), 222 (1975)].
14. Troitskii Yu.V. *Kvantovaya Elektron.*, **2** (11), 2444 (1975) [*Sov. J. Quantum Electron*., **5** (11), 1331 (1975)].
15. Yeh Y., Park S.H. *Opt. Lett*., **37** (4), 626 (2012).
16. Lee L., Hung C.H., Li C.M., You C.W.Y. *Opt.Commun*., **285**, 4395 (2012).
17. Troitskii Yu.V. *Odnochastotnaya generatsiya v gazovykh lazerakh* (Single-Frequency Operation of Gas Lasers) (Novosibirsk: Nauka, 1975).